Telomere Maintenance in Laser Capture Microdissection–Purified Barrett's Adenocarcinoma Cells and Effect of Telomerase Inhibition *In vivo*

Masood A. Shammas,[1] Aamer Qazi,[1] Ramesh B. Batchu,[1] Robert C. Bertheau,[2,3,4] Jason Y.Y. Wong,[3,5] Manjula Y. Rao,[3,4] Madhu Prasad,[1] Diptiman Chanda,[6] Selvarangan Ponnazhagan,[6] Kenneth C. Anderson,[2,3] Christopher P. Steffes,[1] Nikhil C. Munshi,[2,3,4] Immaculata De Vivo,[3,5] David G. Beer,[7] Sergei Gryaznov,[8] Donald W. Weaver,[1] and Raj K. Goyal[3,4]

Abstract

Purpose: The aims of this study were to investigate telomere function in normal and Barrett's esophageal adenocarcinoma (BEAC) cells purified by laser capture microdissection and to evaluate the effect of telomerase inhibition in cancer cells *in vitro* and *in vivo*.

Experimental Design: Epithelial cells were purified from surgically resected esophagi. Telomerase activity was measured by modified telomeric repeat amplification protocol and telomere length was determined by real-time PCR assay. To evaluate the effect of telomerase inhibition, adenocarcinoma cell lines were continuously treated with a specific telomerase inhibitor (GRN163L) and live cell number was determined weekly. Apoptosis was evaluated by Annexin labeling and senescence by β-galactosidase staining. For *in vivo* studies, severe combined immunodeficient mice were s.c. inoculated with adenocarcinoma cells and following appearance of palpable tumors, injected i.p. with saline or GRN163L.

Results: Telomerase activity was significantly elevated whereas telomeres were shorter in BEAC cells relative to normal esophageal epithelial cells. The treatment of adenocarcinoma cells with telomerase inhibitor, GRN163L, led to loss of telomerase activity, reduction in telomere length, and growth arrest through induction of both the senescence and apoptosis. GRN163L-induced cell death could also be expedited by addition of the chemotherapeutic agents doxorubicin and ritonavir. Finally, the treatment with GRN163L led to a significant reduction in tumor volume in a subcutaneous tumor model.

Conclusions: We show that telomerase activity is significantly elevated whereas telomeres are shorter in BEAC and suppression of telomerase inhibits proliferation of adenocarcinoma cells both *in vitro* and *in vivo*.

Authors' Affiliations: [1]Department of Surgery, Wayne State University and Karmanos Cancer Institute, Detroit, Michigan; [2]Dana-Farber Cancer Institute, [3]Harvard Medical School, [4]VA Boston Healthcare System, and [5]Department of Medicine, Brigham and Women's Hospital, Boston, Massachusetts; [6]University of Alabama at Birmingham, Birmingham, Alabama; [7]University of Michigan, Ann Arbor, Michigan, and [8]Geron, Corporation, Menlo Park, California

Received 2/20/08; revised 3/27/08; accepted 3/30/08.

Grant support: NIH-P50-100007 Developmental Research Award (M.A. Shammas); Department of Veterans Affairs Merit Review Awards Research Service and Department of Veterans Affairs Merit Review Awards Epidemiology Service; NIH grants P50-100007 and PO1-78378 (N.C. Munshi); and Karmanos Cancer Institute, Detroit, Michigan.

The costs of publication of this article were defrayed in part by the payment of page charges. This article must therefore be hereby marked *advertisement* in accordance with 18 U.S.C. Section 1734 solely to indicate this fact.

Note: M.A. Shammas, A. Qazi, and R.B. Batchu contributed equally to this work.

Requests for reprints: Raj K. Goyal, Harvard Medical School at Veterans Affairs Medical Center, 1400 VFW Parkway, West Roxbury, MA 02132. Phone: 857-203-5612; E-mail: Raj_goyal@hms.harvard.edu or Masood A. Shammas, Karmanos Cancer Institute/Wayne State University, 615, Hudson Webber Cancer Research Center, 4100 John R. Street, Detroit, MI 48201. Phone: 313-576-8869; E-mail: mshammas@med.wayne.edu.

doi:10.1158/1078-0432.CCR-08-0473

The ends of eukaryotic chromosomes associate with specific DNA binding proteins to form specialized nucleoprotein structures that play a vital role in maintaining genomic integrity by preventing exonucleolytic degradation and end-to-end fusion of chromosomal DNA (1). In humans, the telomeric DNA is composed of few hundred to several thousand repeats of a conserved DNA sequence "TTAGGG" (2–4), which is associated with at least six proteins, TRF1, TRF2, TIN2, HRAP, POT1, and TPP (5), each with a specific role in the maintenance of telomeric DNA length and genomic integrity of a cell.

Telomere length in normal somatic cells shortens with each cell division. Because DNA polymerases require a RNA primer to initiate DNA synthesis, they are unable to replicate the 5′ end of lagging strand of DNA, leading to a loss of 50 to 100 bp of telomeric DNA with each cell division in normal human cells (6). When telomere length reaches below the critical limit of 2 kb, the critically short telomeres are recognized as DNA damage and may lead to either apoptosis and/or cellular senescence (7–9). The length of telomeric DNA may therefore act as a mitotic clock (10), which determines the life span of normal human somatic cells. Although telomeres play a vital

role in the maintenance of genomic integrity and cellular health (11–14), telomere dysfunction or excessive telomere shortening caused by mutation or inherited disorder may result in genetic instability (15) and development of cancer (16). Consistent with these findings, it has been shown that telomere length may serve as a marker for progression and/or prognosis for cancers such as neuroblastoma (17), prostate, colon, breast, brain, head and neck, and lung (18).

Telomere length is maintained by telomerase, an enzyme with a RNA component (TERC) containing a short template for the synthesis of TTAGGG telomere repeats (19) and a polypeptide component with a reverse transcriptase activity (TERT). Telomerase extends telomere length by adding TTAGGG sequences to guanine-rich strand of telomeric DNA. The activity of telomerase depends on posttranslational and posttranscriptional modifications of the protein component (hTERT), including phosphorylation, assembly into telomerase holoenzyme, and its association with other proteins such as p23, and hsp90, etc. (6, 20). Telomerase activity is present in human germ-line cells that maintain their telomere length (21). Conversely, telomerase activity is low or undetectable in normal somatic tissues in which telomeres are not extended and, therefore, undergo progressive shortening with cell division (22). Telomerase knockout mice show a number of abnormalities, including hair graying, alopecia, higher incidence of skin lesions, reduced body weight, delayed healing, diminished hematopoietic reserve, and atrophy of small intestinal cells by generation 3 (23). Additionally, they show hypoproliferative defects in lymphoid, hematopoietic, and gonadal cells by generation 6 (24). Conversely, the induction of telomerase in normal human cells increases their life span in culture (25) and oncogenic conversion in the presence of SV40 T antigen and H-ras (26). Consistent with this, telomerase is reactivated in most immortalized cells (27–31) and cancers (30).

Although a majority of immortal and cancer cells have elevated telomerase activity, a subset of immortal and cancer cell lines lack detectable telomerase activity, and maintain their telomeres through an alternative mechanism (32). Consistent with this, Opitz et al. (33) have shown the immortalization of human primary oral squamous epithelial cells through a mechanism independent of telomerase. However, it has also been shown that human cells can use both telomere maintenance mechanisms, telomerase and an alternative mechanism, at the same time (34).

In cancer cells, telomerase activity is elevated and telomeres are shorter but stable (35, 36). Because telomeres are shorter in cancer cells relative to normal cells whereas telomerase activity is elevated in most cancers but absent or low in normal somatic cells (21, 29, 37), the inhibitors of telomerase activity have a strong potential to be used as anticancer therapeutics, which may inhibit proliferation of tumor cells while having little or no effect on normal cells. Low levels of telomerase activity is also detected in some normal somatic cells such as hematopoietic, peripheral blood, and gastroesophageal cells; however, transient telomerase inhibition may not affect them as telomeres in normal cells are significantly longer than those in cancer. Consistent with this, we have shown that treatment of various cancer (8, 9, 38–40) and immortal (human cell lines; refs. 41, 42) cell lines with a variety of telomerase inhibitors results in the loss of telomerase activity, telomere shortening, and reversal of immortality.

Morales et al. (43) have shown that the expression of RNA component of telomerase (hTR) is increased in surgical specimens of Barrett's esophagus and further elevated in high-grade dysplasia and esophageal adenocarcinoma. Consistent with this report, studies by Lord et al. (44) indicate that transcript levels of catalytic subunit of telomerase (hTERT) are also elevated early at Barrett's esophagus stage with a further up-regulation in specimens of high-grade dysplasia and adenocarcinoma. These studies may indicate that telomerase expression is increased early at Barrett's esophagus stage; however, levels of hTR and hTERT do not reflect telomerase activity, the ability of enzyme to add telomeric repeats. Although hTERT mRNA expression correlates with telomerase activity in many cancers, it does not measure telomerase activity (45), which depends on posttranscriptional and posttranslational modifications of hTERT, including phosphorylation of hTERT protein, assembly into telomerase holoenzyme, and its association with other proteins such as hsp90 and p23, etc. (6, 20).

The aims of this study were to (*a*) assess telomerase activity and telomere length in primary human cells [normal and cancer; Barrett's esophageal adenocarcinoma (BEAC)] purified by laser capture microdissection and (*b*) evaluate the efficacy of a specific telomerase inhibitor, GRN163L, *in vitro* and *in vivo*. We show that BEAC cells purified from surgical specimens by laser capture microdissection (LCM) have significantly elevated telomerase activity and markedly reduced telomeres relative to normal esophageal epithelial cells. The treatment of adenocarcinoma cells with a specific and potent telomerase inhibitor, GRN163L, led to loss of telomerase activity, further reduction in telomere length, and inhibition of cell growth through induction of both the senescence and apoptosis. GRN163L-induced cell death could also be expedited by combination treatment with doxorubicin (a DNA-interacting drug) or ritonavir (a protease inhibitor). Addition of these drugs to cultures pretreated with GRN163L had a significant additive effect on GRN163L-induced cancer cell death. Efficacy of GRN163L was also tested in a murine model in which severe combined immunodeficient mice (SCID) mice were s.c. inoculated with SEG-1 adenocarcinoma cells and, following appearance of palpable tumors, treated with either PBS or GRN163L. A significant reduction in tumor volume was seen in mice treated with the drug.

Materials and Methods

Human tissues. Tissue samples that were immediately processed and frozen at -80°C from surgically resected esophagi bearing various Barrett's esophagus–related lesions, including adenocarcinoma, were used for this study. The protocol for this study is already approved by the institutional review board of the University of Michigan, Ann Arbor, MI. The tissue specimens were coded without use of any of patient private identifiers. For all specimens, only the mucosa containing the columnar epithelium or cancer or normal squamous mucosa was selected by macrodissection. The presence of goblet cells was diagnostic for Barrett's mucosa. The specimens of five normal, one Barrett's, and five BEAC were used for this study and the Barrett's esophagus specimen was from the patient who had cancer. Populations of normal and abnormal cells were isolated by LCM.

Acquisition of target cells with LCM. Target cells from fresh-frozen tissue sections were obtained using the LCM technique as follows: Frozen tissue sections (8 μm) were cut, mounted onto glass slides, fixed

(70% ethanol for 3 min), and stained with hematoxylin. The stained sections were examined under a microscope by an experienced gastrointestinal pathologist and the targeted area, including various Barrett's esophagus–related lesions, was identified according to the standard histopathologic criteria (46). Specialized intestinal metaplasia was defined as specialized columnar epithelium containing well-formed goblet cells whereas BEAC was defined with the breakdown of the basement membrane by dysplastic glands that present within the laminar propria and beyond. Once the targeted glands were identified, the area was marked with a marker and the slide was repositioned for LCM using the Pixcell II LCM System (Arcturus, Inc.), according to the standard protocol (47). The captured cells were placed in an appropriate buffer for subsequent analysis.

Telomere length analysis. Genomic DNA was isolated from captured cells using the QIAamp DNA Micro Kit (Qiagen). Average relative telomere length as represented by the telomere repeat copy number to single copy gene copy number (T/S) ratio was determined using a modified version of a previously described real-time PCR assay on an Applied Biosystems 7900HT Thermocycler (48). Briefly, 5 ng of genomic DNA were dried down in a 384-well plate and resuspended in 10 μL of either the telomere or 36B4 quantitative PCR reaction mixture. Primer sequences of Tel-1, Tel-2, 36B4-U, and 36B4-D were previously described (48). The telomere reaction mixture consisted of 1× Qiagen Quantitect Sybr Green Master Mix, 2.5 mmol/L of DTT, 270 nmol/L of Tel-1, and 900 nmol/L of Tel-2 primer. The reaction proceeded for 1 cycle at 95°C for 5 min, followed by 40 cycles at 95°C for 15 sec and at 54°C for 2 min. The 36B4 reaction consisted of 1× Qiagen Quantitect Sybr Green Master Mix, 300 nmol/L of 36B4U primer, and 500 nmol/L of 36B4D primer. The 36B4 reaction proceeded for one cycle at 95°C for 5 min, followed by 40 cycles at 95°C for 15 sec and at 58°C for 1 min. All samples for both the telomere and 36B4 reactions were done in triplicate. In addition to the samples, each 384-well plate contained a 6-point standard curve from 1.25 to 30 ng using pooled buffy coat–derived genomic DNA. The slope of the standard curve for both the telomere and 36B4 reactions was -3.6 ± 0.2 and the linear correlation coefficient (R^2) value for both reactions was 0.98 and 0.99, respectively. The T/S ratio for each sample was calculated by subtracting the mean 36B4 Ct value from the mean telomere Ct value. The T/S ratio values were then linearized to $2^{-(-dCt)}$.

Assay of telomerase activity. For telomerase activity assays, the cells were immediately lysed in CHAPS lysis buffer (Chemicon International, Inc.) at 50 cells/μL and stored at -150°C. Telomerase activity was measured by an improved version of the original telomeric repeat amplification protocol, using the TRAPeze XL Telomerase Detection Kit (Chemicon International), as previously reported (8, 9, 39). TRAPeze XL is a fluorescence-based highly sensitive assay and provides quantitative analysis of telomerase activity. Using this assay, telomerase activity can be detected in extracts from as few as 100 telomerase-positive cells. In triplicate, cell lysates were mixed with TRAPeze XL reaction mix containing Amplifuor primers and incubated at 30°C for 30 min. Amplified telomerase products were quantitated with FLUOstar OPTIMA Fluorescence Plate Reader (BMG LABTECH). Telomerase activity (in TPG units) was then calculated by comparing the ratio of telomerase products to an internal standard for each lysate, as described by the manufacturer. The assay has a linear range of 1 to 300 TPG units, equivalent to telomerase activity from ~30 to 10,000 control cells.

Telomerase inhibitor GRN163L. GRN163L is a palmitoyl (C16) lipid-attached oligonucleotide (5′-Palm-TAGGGTTAGACAA 3′) targeting the RNA component of telomerase and having a N3′-P5′-thiophosphoramidate backbone.

Cell lines and treatments. Adenocarcinoma cell lines BIC-1, SEG-1, and FLO-1 have been described previously (49). Cells were cultured in DMEM with 10% fetal bovine serum, as described previously (49). Constant numbers of cells were plated in multiple 100-mm dishes; treated with GRN163L at 0.5 to 2.0 mmol/L; and evaluated weekly for cell viability, telomere length, and telomerase activity. Briefly, every week, the cells were harvested and counted, and the viable cell number was confirmed by trypan blue exclusion and 3-(4,5-dimethylthiazol-2-yl)-2,5-diphenyltetrazolium bromide (MTT) assays. Aliquots of cells were separated for various molecular analyses and the remaining cells were replated at the same cell number and at the same concentration of the inhibitor. For combination studies, cells were pretreated with GRN163L for 10 d. Test agents were then added at various concentrations and live cell number was determined at alternate days.

Apoptosis. Following exposure to GRN163L, apoptotic cells were detected by Annexin labeling using FITC-Annexin Apoptosis Detection Kit (Oncogene Research Products). Briefly, the cells treated with GRN163L were harvested and 0.5 mL of cells (1×10^6/mL) was mixed with FITC-Annexin in "binding buffer" and incubated for 15 min at room temperature. A portion of cell suspension (50 μL) was placed onto a glass slide, covered with a coverslip, and viewed immediately using a fluorescence microscope equipped with FITC (green) filter. Approximately 200 cells, representing at least five distinct microscopic fields, were analyzed to assess the fraction of FITC-labeled cells for each sample.

Senescence. One day before this assay, the treated cells were plated on Lab-Tek slides in the presence of mismatch or match (GRN163L) oligonucleotide and the attached cells were stained for β-galactosidase expression, a marker for cellular senescence (50). Briefly, the cells were rinsed thrice with PBS and fixed in 2% formaldehyde and 0.2% glutaraldehyde solution in PBS. The cells were then washed again as described above and stained overnight in solution containing 1 mg/mL X-gal, 40 mmol/L citric acid/sodium phosphate (pH 6), 5 mmol/L potassium ferrocyanide, 150 mmol/L NaCl, and 2 mmol/L $MgCl_2$. The stain was then removed, cells were rinsed with PBS, and staining was viewed under a fluorescence microscope (Olympus).

Murine subcutaneous tumor model. SCID mice were purchased from the National Cancer Institute-Frederick Animal Production area. Maintenance of the animals was carried out following guidelines of the Institutional Animal Care and Use Committee and all experimental procedures were approved by the Institutional Animal Care and Use Committee and the Occupational Health and Safety Department of the University of Alabama at Birmingham. The mice were acclimatized for a week and 3.0×10^6 SEG-1 cells in 100 μL saline were injected s.c. in the interscapular area. Following appearance of palpable tumors, mice were injected i.p. with normal saline alone or GRN163L at concentrations described in the figure legends. Animals were sacrificed when tumors reached 2 mL in volume or when paralysis or major compromise in their quality of life occurred.

Results

LCM significantly enhances the sensitivity of telomerase activity assay. Epithelial cells were purified from tissue specimens of normal and Barrett's esophagi as shown in Fig. 1A, and telomerase activity was measured in these purified cells and also in tissue extracts of the same specimens, using same amount of total protein. Telomerase activity in tissue extracts of normal and Barrett's esophagus was only 3.1 ± 0.9 and 19 ± 4.6 TPG units, respectively. However, the activity in LCM-purified normal and Barrett's esophageal cells was 37.7 ± 5.5 and 197 ± 23.1 TPG units, respectively (Fig. 1B). These data show that telomerase activity is ~10-fold higher in LCM-derived cells relative to that in tissue extracts of the same samples. To investigate if the low activity detected in tissue extracts was due to PCR inhibitors, both the tissue extracts and lysates of LCM-purified Barrett's esophagus cells were diluted and evaluated for telomerase activity. A 10-fold dilution of tissue extract and the lysate of LCM-purified cells of Barrett's esophagus led to 11.4- and 9.2-fold reduction in telomerase activity, respectively.

Telomerase activity is markedly elevated in BEAC relative to normal esophageal epithelial cells. Epithelial cells purified from

tissue specimens of normal, Barrett's adenocarcinoma (BEAC), and commercially obtained primary normal esophageal epithelial cells (HEEC; ScienCell) were lysed at the same cell concentration and evaluated for telomerase activity using TRAPeze XL Telomerase Detection Kit (Chemicon International). The telomerase activity in LCM-purified normal esophageal epithelial cells from three different donors was 41 ± 8 TPG units; consistent with this, the activity in commercially obtained primary normal esophageal epithelial cells (HEEC) was also low (37 ± 3 TPG units; Fig. 1C). A markedly elevated telomerase activity was detected in BEAC (275 ± 20 TPG units; Fig. 1C). Relative to normal esophageal epithelial cells, the activity in BEAC was 7.0 ± 0.5-fold elevated (P = 0.004). These data indicate that telomerase activity is significantly elevated in primary BEAC cells relative to normal esophageal epithelial cells.

Telomeres are consistently shorter in BEAC relative to normal esophageal epithelial cells. We next analyzed telomere length in a panel of LCM-purified normal and BEAC cells. Genomic DNA was isolated using QIAamp DNA Micro Kit (Qiagen) and telomere length was measured by real-time kinetic quantitative PCR (48). Briefly, the PCR reactions for telomere specific (T) and β2-globin control gene specific (S) amplification were set up in separate 96-well plates. Except primers, other conditions, including reagent concentrations, DNA amount, and sample order, were the same for both plates. To monitor the efficiency of PCR reactions, a standard curve spanning at least 0.3 to 5 ng/μL of reference DNA was produced in each 96-well plate. DNA from each sample and reference DNA were tested in triplicate using a total of 12.5 ng DNA per well. PCR amplification reactions were done in a PRISM 7900 Sequence Detection System (Applied Biosystems) using conditions described by Cawthon (48). Analysis of data and determination of telomere length were done using a software (Applied Biosystems), as described (48). The ratio of telomere-specific (T) and single control gene–specific (S) real-time kinetic PCR reactions (T/S ratio) indicated the relative telomere length. The T/S ratio, indicating relative telomere length, ranged from 10.3 to 14.3 in normal cells and 6.2 to 9.2 in BEAC cells, indicating that telomeres in all BEAC specimens were shorter than those in normal samples (Fig. 2A). Average TL was reduced by 38% (P = 0.001) in BEAC relative to the length in normal epithelial cells (Fig. 2B). These results provided a further rationale for investigating the importance of telomerase as a target for the treatment of BEAC.

GRN163L is taken up by adenocarcinoma cells without transfection and inhibits telomerase activity. GRN163L is a palmitoyl (C16) lipid-conjugated oligonucleotide N3′-P5′-thiophosphoramidate targeting template region of RNA component of telomerase (hTR; Fig. 3A). We treated SEG-1 cells with

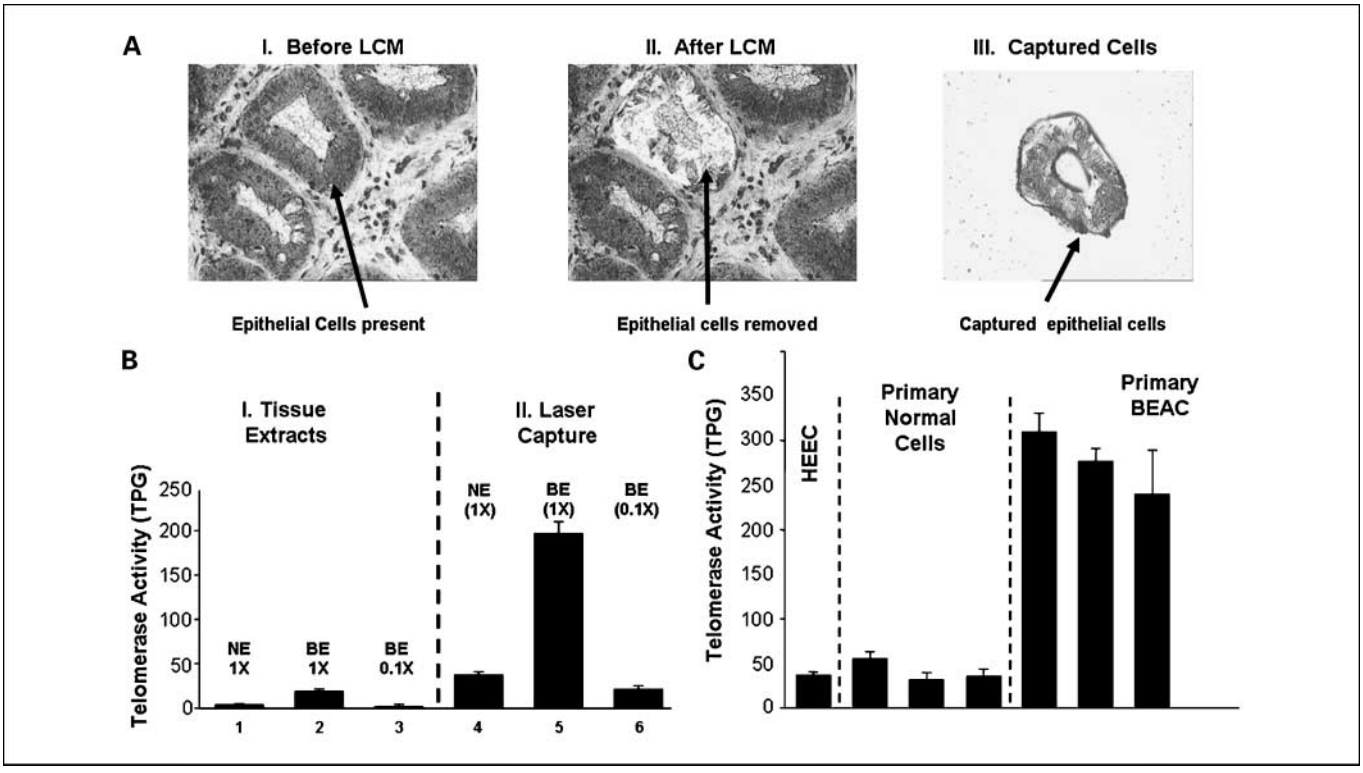

Fig. 1. Telomerase activity in tissue extracts and esophageal epithelial cells isolated by LCM. *A,* isolation of esophageal epithelial cells by LCM. *I,* epithelial cells in a microscopic field before LCM; *II,* the same microscopic field after LCM, showing that epithelial cells have been removed; *III,* the captured epithelial cells. *B,* telomerase activity in tissue extract versus LCM-purified cells. Three normal and three BEAC surgical specimens were processed for evaluation of telomerase activity in LCM and tissue extracts. Each surgical specimen was cut into two portions; one was processed for LCM purification of epithelial cells and the other was used for making the tissue extract. Telomerase activity is shown in the tissue extract, equivalent of 0.6 μg protein, of normal esophagus (*lane 1*); tissue extract, equivalent of 0.6 μg protein, of Barrett's esophagus (*lane 2*); diluted tissue extract, equivalent of 0.06 μg protein, of Barrett's esophagus (*lane 3*); lysate of LCM-purified normal esophageal epithelial cells, equivalent of 0.6 μg protein (*lane 4*); lysate of LCM-purified Barrett's esophagus cells, equivalent of 0.6 μg protein (*lane 5*); and diluted lysate, equivalent of 0.06 μg protein, of LCM-purified Barrett's esophagus cells (*lane 6*). *C,* telomerase activity in defined primary normal and Barrett's adenocarcinoma (BEAC) cells derived by LCM. The activity was measured in the lysates (equivalent of 0.6 μg protein) of normal primary esophageal epithelial cells purchased from ScienCell (HEEC), epithelial cells purified from surgical specimens of normal esophagus from three different patients, and epithelial cells purified from surgical specimens of BEAC from three different patients, using LCM.

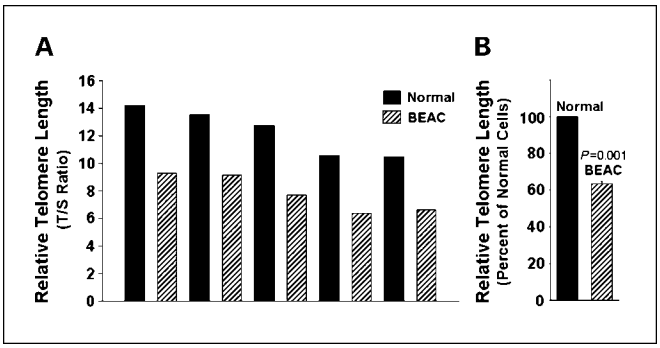

Fig. 2. Telomere length in esophageal epithelial cells isolated from normal and Barrett's adenocarcinoma specimens by LCM. Normal epithelial and BEAC cells were isolated by LCM, genomic DNA was extracted, and telomere length was determined by quantitative PCR. *A,* relative telomere length in primary normal and BEAC cells purified by LCM. *B,* average telomere length in five normal and five BEAC specimens is shown as percent of telomere length in normal cells.

TAMRA-labeled GRN163L at various concentrations and monitored the uptake and intracellular localization at 24 hours using a confocal microscope. As seen by TAMRA (*red*) fluorescence in Fig. 3B, the drug was efficiently taken by SEG-1 cells without any need of a transfection procedure or reagent. The fluorescence was predominantly nuclear. An efficient uptake of GRN163L without any need for transfection reagents was also observed for other adenocarcinoma cell lines BIC-1 and FLO-1 (not shown).

We next evaluated if the uptake of GRN163L was also associated with the inhibition of telomerase activity. We therefore treated SEG-1, FLO-1, and BIC-1 cells with the drug at 0.1, 0.5, 1.0, and 2.0 μmol/L concentrations for 24 hours and evaluated for telomerase activity using TRAPeze XL Telomerase Detection Kit (Intergen). GRN163L at 1 and 2 μmol/L led to near-complete inhibition of telomerase activity in SEG-1 cells (Fig. 3C). Mismatch control oligonucleotide thiophosphoramidate 5′-Palm-TAGGTGTAAGCAA (mismatch bases are underlined, designated as GRN140833) had no effect on growth of these cells at either concentration. Similarly, the treatment with 1 μmol/L of GRN163L led to >95% inhibition of telomerase activity in FLO-1 (Fig. 3D) and BIC-1 cells (not shown). No significant inhibition of telomerase activity was seen at 0.1 μmol/L concentration in any cell line.

Inhibition of telomerase by GRN163L leads to induction of growth arrest in adenocarcinoma cells. Cells were treated with GRN163L or mismatch oligonucleotide GRN140833 and the substrate-attached viable cell number was counted every week. Cell viability was further confirmed by trypan blue exclusion and/or MTT assays. A marked arrest of cell proliferation was observed in all cell lines following treatment with the inhibitor, leading to a gradual decline in viable cell number by 79% to 82% in a span of 2 to 3 weeks. Treatment of SEG-1 cells with the drug at 1 and 2 μmol/L concentrations induced 45% and 80% cell death, respectively, in a period of 21 days (Fig. 4A). Similar induction of cell death was observed following 3-week

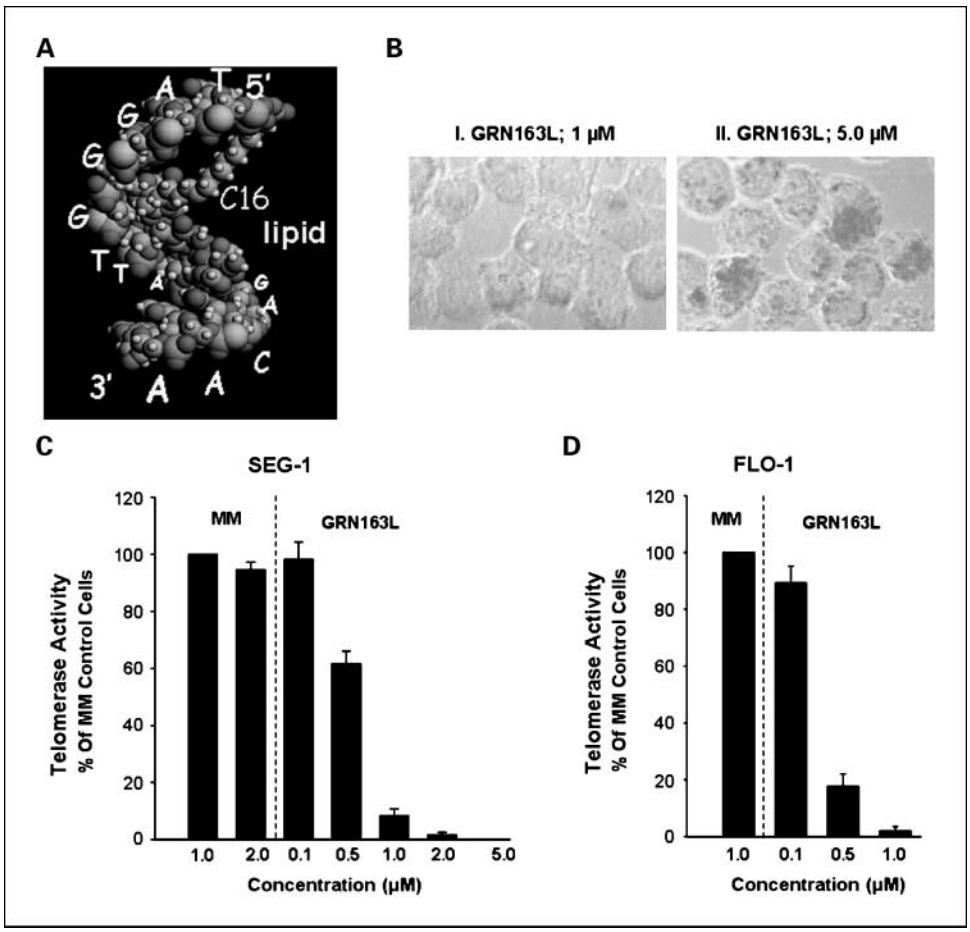

Fig. 3. GRN163L inhibits telomerase activity in adenocarcinoma cells. *A,* structure of GRN163L, a palmitoyl (C16) lipid-attached oligonucleotide targeting RNA component of telomerase. *B,* uptake of GRN163L in SEG-1 cells without any need of transfection. Cells were treated with TAMRA-labeled GRN163L for 24 h and examined by a multiphoton fluorescence microscope. Uptake can be seen as red fluorescence. *C* and *D,* telomerase activity in cells treated with a mismatch control oligonucleotide (*MM*) or GRN163L. SEG-1 (*C*) and FLO-1 (*D*) were treated with GRN163L at various concentrations for 24 h and evaluated for telomerase activity using TRAPeze XL Telomerase Detection Kit.

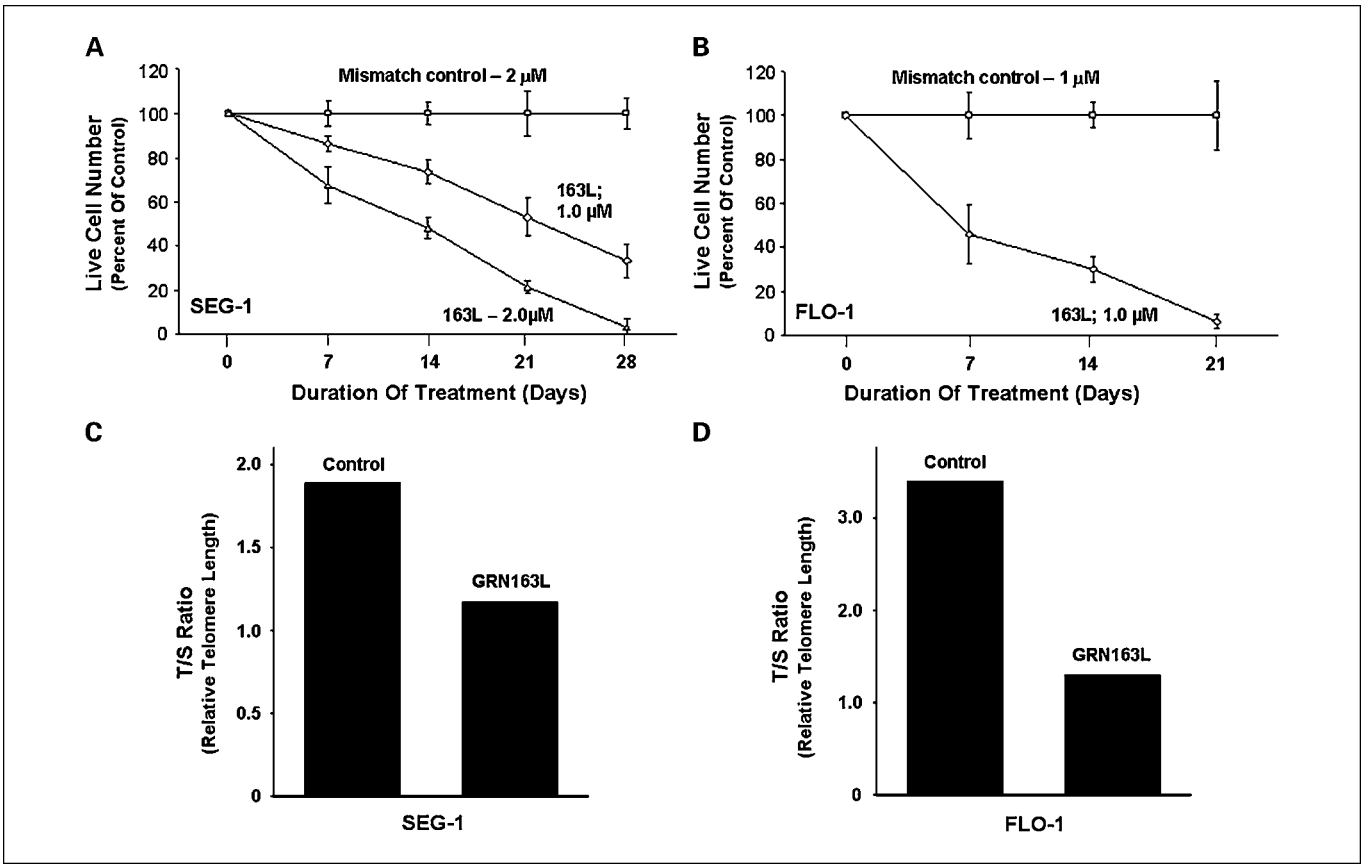

Fig. 4. Effect of GRN163L on growth and telomere length of adenocarcinoma cells. *A* and *B,* cells were cultured in regular growth medium containing GRN163L or mismatch control oligonucleotide at concentrations shown and live cell number was determined at different time points as indicated. Points, mean of three independent experiments; bars, SE. *A,* SEG-1 cells; *B,* FLO-1 cells; *C* and *D,* telomere shortening in cells treated with GRN163L. Cells were treated with mismatch control oligonucleotide or GRN163L at 1 μmol/L for 3 wk and telomere length was examined by quantitative PCR. *C,* relative telomere length in control and GRN163L-treated SEG-1 cells. *D,* relative telomere length in control and GRN163L-treated FLO-1 cells.

treatments of FLO-1 (Fig. 4B) and BIC-1 (not shown). Consistent with telomerase activity data, 1 μmol/L GRN163L was enough to induce a marked (80%) growth inhibition in FLO-1 cells (Fig. 4B).

GRN163L-induced inhibition of telomerase activity is associated with reduction in telomere length. We also analyzed telomere length following exposure of cells to GRN163L using the same real-time kinetic quantitative PCR as described above (48). Telomere length in GRN163L-treated SEG-1 and FLO-1 cells was reduced by 38% and 67%, respectively, relative to cells treated with mismatch control oligonucleotide (Fig. 4C and D). These data indicate that inhibition of telomerase and growth arrest following treatment with GRN163 was also associated with reduction in telomere length.

The nature of cell death following GRN163L treatment. Cell lines were treated with 1 μmol/L GRN163L and evaluated for apoptosis and senescence. Apoptotic cells were detected using an Annexin V-FITC Apoptosis Detection Kit (BD Biosciences). Following 2 weeks of treatment with 2 μmol/L GRN163L, 85 ± 9% of SEG-1 cells stained positive for Annexin V, whereas only 2.4 ± 2% Annexin V–positive cells were detected when the cells were treated with mismatch oligonucleotide (Fig. 5A). Annexin labeling was also detected in a majority (57 ± 3%) of FLO-1 cells treated with drug (Fig. 5B). These data indicate that telomerase inhibition and telomere shortening were associated with induction of apoptosis in treated cells.

GRN163L-treated cells were also evaluated for expression of β-galactosidase, a marker for cell senescence. Interestingly, a large fraction (64 ± 7%) of SEG-1 cells treated with GRN163L also stained positive for β-galactosidase. Moreover, a subset of GRN163L-treated cells also showed typical senescent morphology and became large in size. Such cells, indicated with red arrows, could be seen in SEG-1 (Fig. 5C), FLO-1 (Fig. 5D), and BIC-1 cells (not shown). These data indicate that GRN163L induced both the senescence and apoptosis in adenocarcinoma cells.

Effect of combining GRN163L-mediated telomerase inhibition with other agents. We have also evaluated the effect of other novel agents on GRN163L-induced adenocarcinoma cell death. Of several agents tested, a DNA-interacting drug "doxorubicin" and a protease inhibitor "ritonavir" had a significant additive effect on GRN163L-induced cell death. Addition of ritonavir and doxorubicin to cultures pretreated with GRN163L for 10 days led to ≥80% cell death within 3 days of addition (Fig. 6A), compared with significantly higher viability of cells treated with either drug alone. These data indicate that cancer cell death following inhibition of telomerase can also be expedited by addition of other agents that may affect telomere length by other mechanisms.

***Telomerase inhibitor GRN163L inhibits adenocarcinoma cell growth* in vivo.** The efficacy of GRN163L was shown in a subcutaneous tumor model. Briefly, the SCID mice were s.c. inoculated in the interscapular area with 3.0×10^6 SEG-1 cells and, following appearance of palpable tumors, mice were injected i.p. with saline alone or GRN163L at 45 mg/kg/d. The tumor size in mice treated with 163L was significantly smaller than control (average tumor size in treated mice being >10-fold smaller; $P = 0.03$), indicating a marked efficacy *in vivo*.

Discussion

In this article, we studied telomere maintenance in primary human BEAC and normal esophageal epithelial cells isolated by LCM and evaluated the effect of telomerase inhibition in

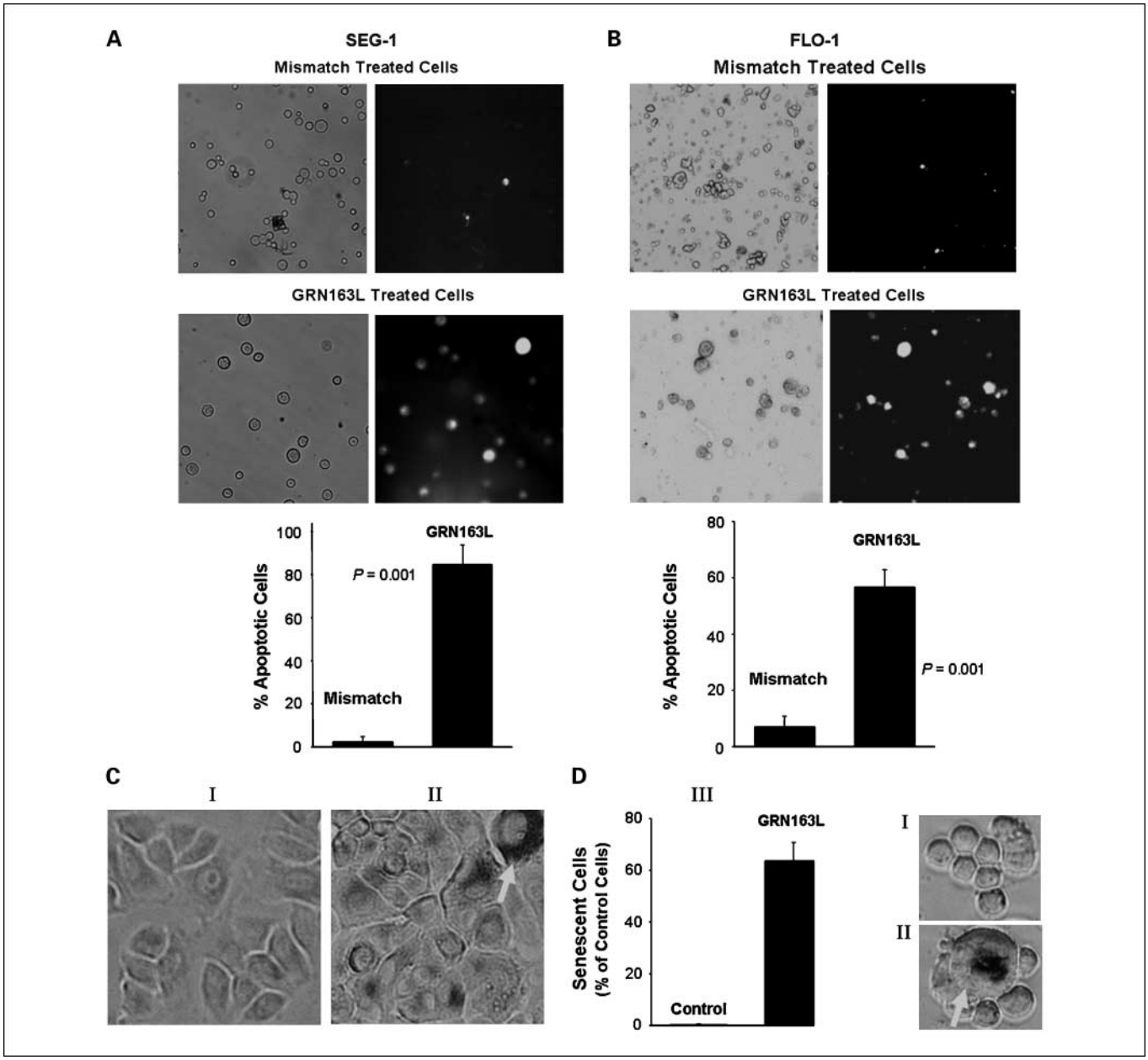

Fig. 5. Apoptosis and senescence in adenocarcinoma cells treated with GRN163L. *A* and *B,* apoptotic cell death in cells treated with GRN163L. The cells treated with control oligonucleotide or GRN163L were harvested; 0.5 mL of cells (1×10^6/mL) were mixed with FITC-Annexin and incubated for 15 min at room temperature. A portion of cell suspension (50 μL) was placed onto a glass slide covered with a coverslip, and FITC-labeled apoptotic cells within the same microscopic field were viewed and photographed by phase contrast or by fluorescence emitted at 518 nm (FITC filter). Apoptotic cells appear bright green. *A,* SEG-1 cells treated with 2 μmol/L control oligonucleotide or GRN163L for 3 wk. *B,* FLO-1 cells, treated with 1 μmol/L control oligonucleotide or GRN163L for 2 wk. Approximately 200 to 300 cells representing five different microscopic fields were evaluated to assess percentage of apoptotic cells, shown as bar graphs in *A* and *B*. *C* and *D,* cells treated with GRN163L were evaluated for expression of β-galactosidase, a marker of cell senescence. *C,* β-galactosidase staining is shown in SEG-1 cells treated with 2 μmol/L control oligonucleotide (*I*) or GRN163L (*II*) for 3 wk. *III,* bar graph showing the percentage of senescent SEG-1 cells. *D,* FLO-1 cells treated with 1 μmol/L control oligonucleotide (*I*) or GRN163L (*II*) for 2 wk. Arrows (*C* and *D*), cells with typical senescent morphology.

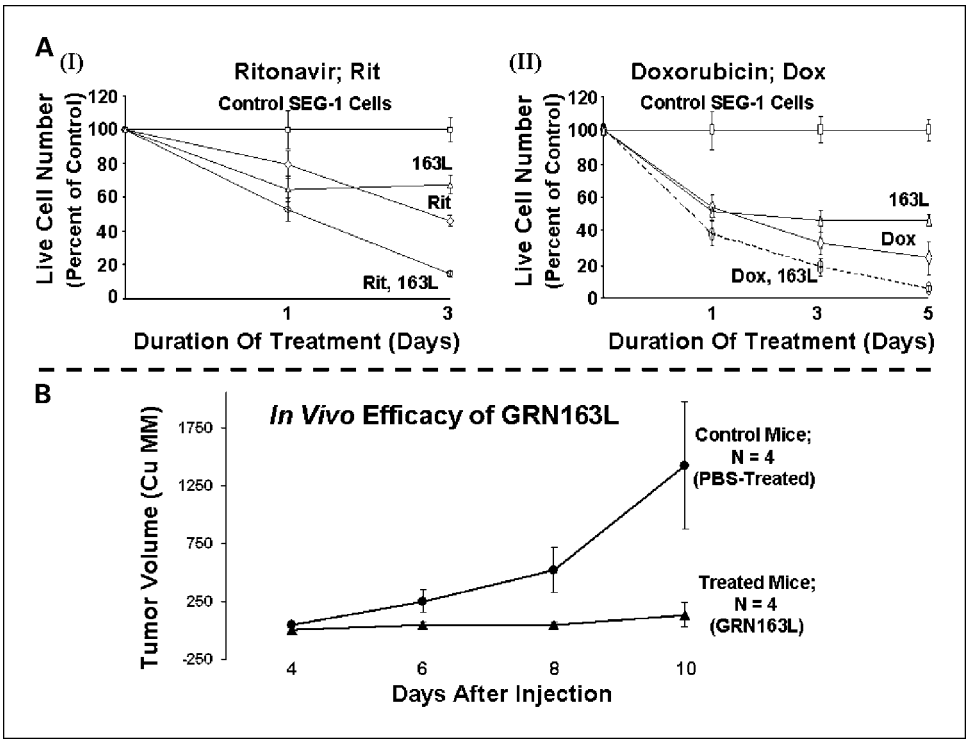

Fig. 6. Efficacy of GRN163L in combination with other agents and in a subcutaneous tumor model. *A,* SEG-1 cells were treated with 2 μmol/L mismatch control oligonucleotide or GRN163L for 10 d and the cells in each treatment flask were then divided into two aliquots. Cells were then cultured either in the presence of mismatch or match (GRN163L) oligonucleotides alone or with addition of ritonavir (2 μmol/L; *I*) or doxorubicin (2 nmol/L; *II*). Live cell number was determined at different time points. *B, in vivo* efficacy of GRN163L in a subcutaneous tumor model. SCID mice were inoculated s.c. in the interscapular area with 3.0×10^6 SEG-1 cells; following the appearance of tumors, the mice were treated i.p. with saline alone or GRN163L 45 mg/kg/d.

three different adenocarcinoma cell lines and in a subcutaneous tumor model using SCID mice. We have shown that (*a*) telomerase activity assays conducted in tissue extracts can produce inaccurate results whereas the assays conducted in LCM-purified specimens are more accurate and reliable; (*b*) telomerase activity is significantly elevated whereas telomeres are significantly shorter in BEAC relative to normal esophageal epithelial cells; (*c*) GRN163L, a lipid -conjugated oligonucleotide telomerase template antagonist, is efficiently taken up by adenocarcinoma cells without any transfection and leads to inhibition of telomerase activity within 24 hours; (*d*) inhibition of telomerase activity is associated with growth arrest, reduction in telomere length, and induction of both the senescence and apoptosis; (*e*) a significant additive effect of doxorubicin and ritonavir was observed on GRN163L-induced growth inhibition; and (*f*) i.p. injections of GRN163L caused a significant reduction in tumor size *in vivo*.

A large discrepancy has been reported for telomerase activity in normal and Barrett's esophagi (51–54) and for the activity observed in surgical and endoscopic biopsy specimens (51). The major cause of this controversy is the fact that these studies have been conducted on tissue extracts contaminated with varying proportions of connective tissue cells. These contaminating cells do not only dilute the lysate but may also have an inhibitory effect on telomerase activity. Bachor et al. (51) have also proposed that the discrepancy arises because of contaminating connective tissue, which is more in surgically obtained specimens and less in superficial biopsies. Consistent with this, it has been shown that removal of dermis from epidermis led to an easier detection of telomerase activity in human skin (55). In an attempt to resolve the discrepancy, we have evaluated and compared telomerase activity in tissue extracts and LCM-purified primary epithelial cells from normal and Barrett's esophagi. As shown in Fig. 1, the telomerase activity was ~10-fold higher in LCM-derived cells relative to that in tissue extracts of the same samples, containing the same amount of protein. The most likely explanation of this observation is that the activity in tissue extracts is substantially diluted because of the contaminating (connective tissue, blood vessels, nerve fibers, and smooth muscle) cells in mucosal tissue. Alternatively, the low telomerase activity detected in tissue extracts could also be due to the presence of PCR inhibitors. However, if this is true, the dilution of the samples should lead to an increase in activity. We therefore diluted both the tissue extracts and LCM samples and evaluated them for telomerase activity. The dilution did not increase; however, decreased telomerase activity and the extent of decline were consistent with the linear standard curve generated from dilutions of a control template. It is therefore less likely that the low telomerase activity detected in tissue extracts in these experiments was due to the presence of PCR inhibitors. We therefore conclude that telomerase assays conducted in tissue extracts, containing varying proportions of contaminating cells, may produce inaccurate results because of the dilution effect. Purification of the specific cells under investigation can avoid all these problems and variables. We would also like to caution that the data shown in Fig. 1B indicate the importance of LCM purification but may not confirm that telomerase activity is elevated in Barrett's esophagi, in general, because of insufficient sample size.

We therefore studied both the telomerase activity and telomere length in laser captured cells. Normal squamous epithelial cells were used as control for BEAC. It has been debatable as to what the appropriate control cells are for Barrett's esophagus. Although Barrett's esophagus cells are columnar, they do not arise from either gastric or intestinal cells. We elected normal squamous epithelial cells as controls and found that telomerase activity is significantly elevated in BEAC. This is consistent with earlier reports of increased telomerase RNA (43) and catalytic

subunit of telomerase (44) in Barrett's adenocarcinoma. Our data also show that telomeres are consistently shorter in BEAC relative to normal esophageal epithelial cells. This is also consistent with the observations of Finley et al. (56), indicating shorter telomeres in BEAC relative to those in epithelial cells from gastroesophageal reflux disease patients. Elevated telomerase activity and shorter telomeres have also been reported in multiple myeloma (40), B-cell chronic lymphocytic leukemia (57), nonhematopoietic cancers such as hepatocellular carcinoma (58), breast cancer (59), and prostate cancer (60).

Although a variety of agents have been shown to inhibit telomerase activity and block proliferation of cancer cells (8, 9, 38, 42, 61–66), very few have been proven to be both specific and suitable for *in vivo* delivery and utilization. The telomerase inhibitor (GRN163L) used in this study is a thio-phosphoramidate oligonucleotide complementary to the template region of the RNA subunit of telomerase (hTERC). This oligonucleotide has a lipid (C_{16}) moiety attached to it, which facilitates the uptake of this molecule in human cells without any need of a transfection procedure or reagent. Using TAMRA-labeled GRN163L, we have shown that this drug is efficiently taken up by human adenocarcinoma cells without any transfection within 24 hours of treatment. Uptake of drug was associated with loss of telomerase activity and growth arrest after a lag period of 3 to 4 weeks. Although for cancers such as cervical cancer, the inhibition of telomerase induces apoptosis within a few days without any requirement of telomere shortening (67), the cell death in a majority of cancer cells occurs after a lag period of a few weeks, which is probably required for reduction of telomere length below critical limit (8, 9, 38, 39, 42, 68). Because the treatment of adenocarcinoma cells with GRN163L was associated with both the lag period and reduction in telomere length, it seems that growth arrest was probably induced by short telomeres.

Critically short telomeres are recognized as DNA damage and therefore activate mechanisms leading to apoptotic cell death or replicative senescence. Consistent with this, the inhibitors of telomerase have been shown to induce apoptotic cell death (9, 38, 39, 69, 70) or both the apoptosis and senescence (8, 69) in different cancer cell lines. In our study, the adenocarcinoma cells treated with GRN163L stained positive for not only Annexin V but also for β-galactosidase, indicating that growth inhibition in these cells was associated with induction of both the senescence and apoptosis. Induction of both the senescence and apoptosis in adenocarcinoma cells following inhibition of telomerase is consistent with our earlier observations (39). However, we would caution that the data do not show that both the senescence and apoptosis were induced simultaneously. Senescence may have preceded apoptosis following inhibition of telomerase, as observed by Herbert at al. (69), in immortal breast epithelial cell line. This is quite consistent with our data showing senescence in 64% and apoptosis in 85% of treated SEG-1 cells.

We have also shown that growth inhibition following exposure of adenocarcinoma cells to a telomerase inhibitor can be significantly expedited by combination therapy with other agents affecting telomerase or telomeres. The rationale of doing a combination study was to first initiate the destruction of telomeric DNA in cancer cells by treating with a specific inhibitor (GRN163L) and then expedite the degradation of vulnerable telomeres by a very brief exposure to an agent, which may be less specific, but could significantly expedite the destruction of already eroding telomeres through different mechanisms. We therefore chose a number of potential agents and evaluated their effect on SEG-1 cells pretreated with GRN163L. Ritonavir and doxorubicin were found to give a significant additive effect, indicating the possibility of combination therapy with GRN163L. The *in vivo* efficacy of GRN163L was shown in a murine tumor model in which SCID mice were inoculated in the interscapular area with SEG-1 adenocarcinoma cells and following appearance of palpable tumors, mice were injected i.p. with either PBS alone or GRN163L. The dose (45 mg/kg/d) of GRN163L used has been shown by us previously to be nontoxic and effective in two different tumor models of SCID mice (71). Average tumor size in the mice treated with the drug was >10-fold smaller than that in control mice ($P = 0.03$), without evidence of toxicity, indicating a remarkable efficacy *in vivo*.

In summary, we have shown that telomerase activity assays conducted in tissue extracts may produce inaccurate results and propose that the activity assays should be conducted in the lysates of cells purified by LCM. We have also shown that telomerase activity is significantly elevated whereas telomere length is significantly shorter in primary epithelial cells derived from tissue specimens of BEAC relative to normal esophageal epithelial cells. GRN163L, a lipid-conjugated oligonucleotide thio-phosphoramidate targeting RNA component of telomerase, is efficiently taken up by human adenocarcinoma cells without any need of a transfection reagent/procedure, inhibits telomerase activity, and induces telomere shortening and growth inhibition by induction of both cellular senescence and apoptosis. The growth inhibition following treatment with GRN163L could also be expedited by a combination therapy with other drugs. Finally, the efficacy of GRN163L has also been shown *in vivo*. These data show that telomerase is a potential target for BEAC and GRN163L is a potent and specific telomerase inhibitor that, either alone or in combination with agents such as ritonavir and doxorubicin, is suited for *in vivo* utilization in human clinical trials.

Disclosure of Potential Conflicts of Interest

S. Gryaznov is employed by Geron Corporation and is co-inventor of GRN163L.

References

1. Day JP, Marder BA, Morgan WF. Telomeres and their possible role in chromosome stabilization. Environ Mol Mutagen 1993;22:245–9.
2. Allshire RC, Gosden JR, Cross SH, et al. Telomeric repeat from *T. thermophila* cross hybridizes with human telomeres. Nature 1988;332:656–9.
3. de Lange T, Shiue L, Myers RM, et al. Structure and variability of human chromosome ends. Mol Cell Biol 1990;10:518–27.
4. Moyzis RK, Buckingham JM, Cram LS, et al. A highly conserved repetitive DNA sequence, (TTAGGG)n, present at the telomeres of human chromosomes. Proc Natl Acad Sci U S A 1988;85:6622–6.
5. Matulic M, Sopta M, Rubelj I. Telomere dynamics: the means to an end. Cell Prolif 2007;40:462–74.
6. Cong YS, Wright WE, Shay JW. Human telomerase and its regulation. Microbiol Mol Biol Rev 2002;66:407–25, table of contents.
7. Akiyama M, Hideshima T, Munshi NC, Anderson KC. Telomerase inhibitors as anticancer therapy. Curr Med Chem Anti-Canc Agents 2002;2:567–75.
8. Shammas MA, Koley H, Batchu RB, et al. Telomerase inhibition by siRNA causes senescence and apoptosis in Barrett's adenocarcinoma cells: mechanism and therapeutic potential. Mol Cancer 2005;4:24.
9. Shammas MA, Koley H, Beer DG, Li C, Goyal RK, Munshi NC. Growth arrest, apoptosis, and telomere

shortening of Barrett's-associated adenocarcinoma cells by a telomerase inhibitor. Gastroenterology 2004;126:1337–46.
10. Harley CB. Telomere loss: mitotic clock or genetic time bomb? Mutat Res 1991;256:271–82.
11. Blasco MA, Lee HW, Hande MP, et al. Telomere shortening and tumor formation by mouse cells lacking telomerase RNA [see comments]. Cell 1997;91:25–34.
12. Collins K. Mammalian telomeres and telomerase. Curr Opin Cell Biol 2000;12:378–83.
13. Ducray C, Pommier JP, Martins L, Boussin FD, Sabatier L. Telomere dynamics, end-to-end fusions and telomerase activation during the human fibroblast immortalization process. Oncogene 1999;18:4211–23.
14. McEachern MJ, Krauskopf A, Blackburn EH. Telomeres and their control. Annu Rev Genet 2000;34:331–58.
15. De Lange T. Telomere-related genome instability in cancer. Cold Spring Harbor Symp Quant Biol 2005;70:197–204.
16. Meeker AK. Telomeres and telomerase in prostatic intraepithelial neoplasia and prostate cancer biology. Urol Oncol 2006;24:122–30.
17. Ohali A, Avigad S, Ash S, et al. Telomere length is a prognostic factor in neuroblastoma. Cancer 2006;107:1391–9.
18. Bisoffi M, Heaphy CM, Griffith JK. Telomeres: prognostic markers for solid tumors. Int J Cancer 2006;119:2255–60.
19. Blackburn EH. Telomerases. Annu Rev Biochem 1992;61:113–29.
20. Aisner DL, Wright WE, Shay JW. Telomerase regulation: not just flipping the switch. Curr Opin Genet Dev 2002;12:80–5.
21. Kim NW, Piatyszek MA, Prowse KR, et al. Specific association of human telomerase activity with immortal cells and cancer [see comments]. Science 1994;266:2011–5.
22. Harley CB, Futcher AB, Greider CW. Telomeres shorten during ageing of human fibroblasts. Nature 1990;345:458–60.
23. Rudolph KL, Chang S, Lee HW, et al. Longevity, stress response, and cancer in aging telomerase-deficient mice. Cell 1999;96:701–12.
24. Lee HW, Blasco MA, Gottlieb GJ, Horner JW II, Greider CW, DePinho RA. Essential role of mouse telomerase in highly proliferative organs. Nature 1998;392:569–74.
25. Bodnar AG, Ouellette M, Frolkis M, et al. Extension of life-span by introduction of telomerase into normal human cells [see comments]. Science 1998;279:349–52.
26. Hahn WC, Counter CM, Lundberg AS, Beijersbergen RL, Brooks MW, Weinberg RA. Creation of human tumour cells with defined genetic elements [see comments]. Nature 1999;400:464–8.
27. Avilion AA, Piatyszek MA, Gupta J, Shay JW, Bacchetti S, Greider CW. Human telomerase RNA and telomerase activity in immortal cell lines and tumor tissues. Cancer Res 1996;56:645–50.
28. Counter CM, Avilion AA, LeFeuvre CE, et al. Telomere shortening associated with chromosome instability is arrested in immortal cells which express telomerase activity. EMBO J 1992;11:1921–9.
29. Shay JW. Telomerase in human development and cancer. J Cell Physiol 1997;173:266–70.
30. Shay JW, Bacchetti S. A survey of telomerase activity in human cancer. Eur J Cancer 1997;33:787–91.
31. Shay JW, Wright WE. The reactivation of telomerase activity in cancer progression. Trends Genet 1996;12:129–31.
32. Bryan TM, Englezou A, Gupta J, Bacchetti S, Reddel RR. Telomere elongation in immortal human cells without detectable telomerase activity. EMBO J 1995;14:4240–8.
33. Opitz OG, Suliman Y, Hahn WC, Harada H, Blum HE, Rustgi AK. Cyclin D1 overexpression and p53 inactivation immortalize primary oral keratinocytes by a telomerase-independent mechanism. J Clin Invest 2001;108:725–32.
34. Cerone MA, Londono-Vallejo JA, Bacchetti S. Telomere maintenance by telomerase and by recombination can coexist in human cells. Hum Mol Genet 2001;10:1945–52.
35. Engelhardt M, Martens UM. The implication of telomerase activity and telomere stability for replicative aging and cellular immortality (Review). Oncol Rep 1998;5:1043–52.
36. Wai LK. Telomeres, telomerase, and tumorigenesis—a review. MedGenMed 2004;6:19.
37. Broccoli D, Young JW, de Lange T. Telomerase activity in normal and malignant hematopoietic cells. Proc Natl Acad Sci U S A 1995;92:9082–6.
38. Masood A, Shammas MA, Shmookler Reis RJ, et al. Telomerase inhibition and cell growth arrest following telomestatin treatment in multiple myeloma. Clin Cancer Res 2004;10:770–6.
39. Shammas MA, Reis RJ, Li C, et al. Telomerase inhibition and cell growth arrest after telomestatin treatment in multiple myeloma. Clin Cancer Res 2004;10:770–6.
40. Shammas MA, Shmookler Reis RJ, Akiyama M, et al. Telomerase inhibition and cell growth arrest by G-quadruplex interactive agent in multiple myeloma. Mol Cancer Ther 2003;2:825–33.
41. Shammas MA, Liu X, Gavory G, Raney KD, Balasubramanian S, Shmookler Reis RJ. Targeting the single-strand G-rich overhang of telomeres with PNA inhibits cell growth and induces apoptosis of human immortal cells. Exp Cell Res 2004;295:204–14.
42. Shammas MA, Simmons CG, Corey DR, Reis RJ. Telomerase inhibition by peptide nucleic acids reverses 'immortality' of transformed human cells. Oncogene 1999;18:6191–200.
43. Morales CP, Lee EL, Shay JW. *In situ* hybridization for the detection of telomerase RNA in the progression from Barrett's esophagus to esophageal adenocarcinoma. Cancer 1998;83:652–9.
44. Lord RV, Salonga D, Danenberg KD, et al. Telomerase reverse transcriptase expression is increased early in the Barrett's metaplasia, dysplasia, adenocarcinoma sequence. J Gastrointest Surg 2000;4:135–42.
45. Swiggers SJ, Nibbeling HA, Zeilemaker A, Kuijpers MA, Mattern KA, Zijlmans JM. Telomerase activity level, but not hTERT mRNA and hTR level, regulates telomere length in telomerase-reconstituted primary fibroblasts. Exp Cell Res 2004;297:434–43.
46. Huang Q, Yu C, Klein M, Fang J, Goyal RK. DNA index determination with Automated Cellular Imaging System (ACIS) in Barrett's esophagus: comparison with CAS 200. BMC Clin Pathol 2005;5:7.
47. Ohyama H, Zhang X, Kohno Y, et al. Laser capture microdissection-generated target sample for high-density oligonucleotide array hybridization. Biotechniques 2000;29:530–6.
48. Cawthon RM. Telomere measurement by quantitative PCR. Nucleic Acids Res 2002;30:e47.
49. Aggarwal S, Taneja N, Lin L, Orringer MB, Rehemtulla A, Beer DG. Indomethacin-induced apoptosis in esophageal adenocarcinoma cells involves upregulation of Bax and translocation of mitochondrial cytochrome C independent of COX-2 expression. Neoplasia 2000;2:346–56.
50. Dimri GP, Lee X, Basile G, et al. A biomarker that identifies senescent human cells in culture and in aging skin *in vivo*. Proc Natl Acad Sci U S A 1995;92:9363–7.
51. Bachor C, Bachor OA, Boukamp P. Telomerase is active in normal gastrointestinal mucosa and not up-regulated in precancerous lesions. J Cancer Res Clin Oncol 1999;125:453–60.
52. Barclay JY, Morris A, Nwokolo CU. Telomerase, hTERT and splice variants in Barrett's oesophagus and oesophageal adenocarcinoma. Eur J Gastroenterol Hepatol 2005;17:221–7.
53. Going JJ, Fletcher-Monaghan AJ, Neilson L, et al. Zoning of mucosal phenotype, dysplasia, and telomerase activity measured by telomerase repeat assay protocol in Barrett's esophagus. Neoplasia 2004;6:85–92.
54. Yoneyama K, Aoyama N, Koizumi H, Tamai S. [Telomerase activity in esophageal carcinoma and lesions unstained with Lugol's solution]. Nippon Rinsho 1998;56:1181–5.
55. Harle-Bachor C, Boukamp P. Telomerase activity in the regenerative basal layer of the epidermis inhuman skin and in immortal and carcinoma-derived skin keratinocytes. Proc Natl Acad Sci U S A 1996;93:6476–81.
56. Finley JC, Reid BJ, Odze RD, et al. Chromosomal instability in Barrett's esophagus is related to telomere shortening. Cancer Epidemiol Biomarkers Prev 2006;15:1451–7.
57. Bechter OE, Eisterer W, Pall G, Hilbe W, Kuhr T, Thaler J. Telomere length and telomerase activity predict survival in patients with B cell chronic lymphocytic leukemia. Cancer Res 1998;58:4918–22.
58. Ohashi K, Tsutsumi M, Kobitsu K, et al. Shortened telomere length in hepatocellular carcinomas and corresponding background liver tissues of patients infected with hepatitis virus. Jpn J Cancer Res 1996;87:419–22.
59. Odagiri E, Kanada N, Jibiki K, Demura R, Aikawa E, Demura H. Reduction of telomeric length and c-erbB-2 gene amplification in human breast cancer, fibroadenoma, and gynecomastia. Relationship to histologic grade and clinical parameters. Cancer 1994;73:2978–84.
60. Sommerfeld HJ, Meeker AK, Piatyszek MA, Bova GS, Shay JW, Coffey DS. Telomerase activity: a prevalent marker of malignant human prostate tissue. Cancer Res 1996;56:218–22.
61. Fu W, Begley JG, Killen MW, Mattson MP. Anti-apoptotic role of telomerase in pheochromocytoma cells. J Biol Chem 1999;274:7264–71.
62. Nakajima A, Tauchi T, Sashida G, et al. Telomerase inhibition enhances apoptosis in human acute leukemia cells: possibility of antitelomerase therapy. Leukemia 2003;17:560–7.
63. Seimiya H, Oh-hara T, Suzuki T, et al. Telomere shortening and growth inhibition of human cancer cells by novel synthetic telomerase inhibitors MST-312, MST-295, and MST-1991. Mol Cancer Ther 2002;1:657–65.
64. Munshi NC, Hideshima T, Carrasco D, et al. Identification of genes modulated in multiple myeloma using genetically identical twin samples. Blood 2004;103:1799–806.
65. Sumi M, Tauchi T, Sashida G, et al. A G-quadruplex-interactive agent, telomestatin (SOT-095), induces telomere shortening with apoptosis and enhances chemosensitivity in acute myeloid leukemia. Int J Oncol 2004;24:1481–7.
66. Tauchi T, Shin-Ya K, Sashida G, et al. Activity of a novel G-quadruplex-interactive telomerase inhibitor, telomestatin (SOT-095), against human leukemia cells: involvement of ATM-dependent DNA damage response pathways. Oncogene 2003;22:5338–47.
67. Yatabe N, Kyo S, Kondo S, et al. 2–5A antisense therapy directed against human telomerase RNA inhibits telomerase activity and induces apoptosis without telomere impairment in cervical cancer cells. Cancer Gene Ther 2002;9:624–30.
68. Akiyama M, Hideshima T, Shammas MA, et al. Effects of oligonucleotide N3′→P5′ thio-phosphoramidate (GRN163) targeting telomerase RNA in human multiple myeloma cells. Cancer Res 2003;63:6187–94.
69. Herbert BS, Pongracz K, Shay JW, Gryaznov SM. Oligonucleotide N3′→P5′ phosphoramidates as efficient telomerase inhibitors. Oncogene 2002;21:638–42.
70. Herbert BS, Sanders BG, Kline K. *N*-(4-Hydroxyphenyl) retinamide activation of transforming growth factor-β and induction of apoptosis in human breast cancer cells. Nutr Cancer 1999;34:121–32.
71. Shammas MA, Koley H, Bertheau RC, et al. Telomerase inhibitor GRN163L inhibits myeloma cell growth *in vitro* and *in vivo*. Leukemia Epub 2008 May 1.